ISSN 1674-1056
http://cpb.iphy.ac.cn
http://iopscience.iop.org/cpb
中国物理 B
Chinese Physics
中国物理 Chinese Physics B

Novel potential energy surface-based quantum dynamics of ion-molecule reaction $O^+ + D_2 \rightarrow OD^+ + D$

Xian-Long Wang(王宪龙), Feng Gao(高峰), Shou-Bao Gao(高守宝), Lu-Lu Zhang(张路路), Yu-Zhi Song(宋玉志), Qing-Tian Meng(孟庆田)
Citation: Chin. Phys. B . 2018, 27(4): 043104. **doi:** 10.1088/1674-1056/27/4/043104

Journal homepage: http://cpb.iphy.ac.cn; http://iopscience.iop.org/cpb

What follows is a list of articles you may be interested in

State-to-state dynamics of $F(^2P)+HO(^2\Pi) \rightarrow O(^3P)+HF(^1\Sigma^+)$ reaction on $1^3A''$ potential energy surface

Juan Zhao(赵娟), Hui Wu(吴慧), Hai-Bo Sun(孙海波), Li-Fei Wang(王立飞)
Chin. Phys. B . 2018, 27(2): 023102. **doi:** 10.1088/1674-1056/27/2/023102

Wetting and coalescence of the liquid metal on the metal substrate

Zhen-Yang Zhao(赵珍阳), Tao Li(李涛), Yun-Rui Duan(段云瑞), Zhi-Chao Wang(王志超), Hui Li(李辉)
Chin. Phys. B . 2017, 26(8): 083104. **doi:** 0.1088/1674-1056/26/8/083104

State-to-state quantum dynamics of $N(^2D)+HD$ (v=0, j=0) reaction

Yong Zhang(张勇)
Chin. Phys. B . 2016, 25(12): 123104. **doi:** 10.1088/1674-1056/25/12/123104

State-to-state quantum dynamics of the $N(^4S)+H_2$ $(X^1\Sigma^+) \rightarrow NH(X^3\Sigma^-)+H(^2S)$ reaction and its reaction mechanism analysis

Zhang Jing, Gao Shou-Bao, Wu Hui, Meng Qing-Tian
Chin. Phys. B . 2015, 24(8): 083104. **doi:** 10.1088/1674-1056/24/8/083104

A typical slow reaction $H(^2S)+S_2(X^3\Sigma_g^-) \rightarrow SH(X^2\Pi)+S(^3P)$ on a new surface：Quantum dynamics calculations

Wei Wei, Gao Shou-Bao, Sun Zhao-Peng, Song Yu-Zhi, Meng Qing-Tian
Chin. Phys. B . 2014, 23(7): 073101. **doi:** 10.1088/1674-1056/23/7/073101

Novel potential energy surface-based quantum dynamics of ion–molecule reaction $O^+ + D_2 \rightarrow OD^+ + D$*

Xian-Long Wang(王宪龙), Feng Gao(高峰), Shou-Bao Gao(高守宝), Lu-Lu Zhang(张路路), Yu-Zhi Song(宋玉志), and Qing-Tian Meng(孟庆田)†

School of Physics and Electronics, Shandong Normal University, Jinan 250358, *China*

(Received 18 December 2017; revised manuscript received 16 January 2018; published online 10 March 2018)

According to a novel electronic ground-state potential energy surface of $H_2O^+(X^4A'')$, we calculate the reaction probabilities and the integral cross section for the titled reaction $O^+ + D_2 \rightarrow OD^+ + D$ by the Chebyshev wave packet propagation method. The reaction probabilities in a collision-energy range of 0.0 eV–1.0 eV show an oscillatory structure for the $O^+ + D_2$ reaction due to the existence of the potential well. Compared with the results of Martínez *et al.*, the present integral cross section is large, which is in line with experimental data.

Keywords: quantum dynamics, Chebyshev wave packet propagation, $O^+ + D_2$

PACS: 31.15.xv, 34.50.–s, 03.67.Lx **DOI:** 10.1088/1674-1056/27/4/043104

1. Introduction

The ion–molecule reaction is of fundamental interest to the interstellar media, plasmas, planetary ionospheres and combustion processes.[1,2] As an ion–diatomic molecule reaction, $O^+ + H_2 \rightarrow OH^+ + H$ system has been playing an increasingly significant role in both the planetary ionospheres and the earth ionosphere. It can also be served as a typical three-atom reaction system in the field of ion–molecule reaction dynamics. So the $O^+ + H_2 \rightarrow OH^+ + H$ reaction and its isotopic variant reaction $O^+ + D_2 \rightarrow OD^+ + D$ have been investigated extensively both experimentally and theoretically.[3–10]

Experimentally, Fehsenfeld *et al.*[3] have measured the rate constant (300 K) for the reactions in which the positive ion such as O^+, N^+, Ar^+, etc. extracts a hydrogen atom from H_2 in a pulsed-discharge, flowing-afterglow reaction tube. Compared with the ion–molecule reactions performed by Smith *et al.*[4] with the similar species at the same temperature using the selected ion flow tube techniques, the rate constant obtained is a little bit big. While for the isotopic variant reaction $O^+ + D_2 \rightarrow OD^+ + D$, Burley *et al.*[5] used the ion beam mass spectrometry to examine the kinetic energy, the total reaction cross sections and the intra-molecular isotope branching ratio, and the results are in excellent agreement with those predicted by the Langevin–Gioumousis–Stevenson model.[6]

Theoretically, Martínez *et al.*[7] constructed a global potential energy surface (PES) of the $H_2O^+(X^4A'')$ system, and using the quasi-classical trajectory (QCT)[8,9] method they obtained the integral cross sections (ICSs) and rate constants at temperatures in a range of 200 K–1400 K for the $O^+ + D_2 \rightarrow OD^+ + D$ reaction, which are in excellent agreement with the experimental results cited from Burley *et al.*'s paper.[5] In 2006, Martínez *et al.*[10] calculated the ICS of the $O^+ + D_2 \rightarrow OD^+ + D$ reaction by the time-dependent real wave packet method within the helicity decoupling approximation,[11] which reinforces the adequacy of the *ab initio* analytical PES used. Bulut *et al.*[12] have obtained the ICS and the rate constant of state-to-state quantum dynamics of reaction $O^+ + H_2$ by the time-dependent wave packet-Coriolis coupling (TDWP-CC) calculations.

In 2015, Song *et al.*[13] constructed a novel electronic ground-state PES of $H_2O^+(X^4A'')$. According to the scanning of this PES, the minimum energy path (MEP) of $O^+(^4S) + H_2(X^1\Sigma_g^+) \rightarrow OH^+(X^3\Sigma^-) + H(^2S)$ is plotted in Fig. 1. According to this PES,[13] we have performed the dynamic calculation of relevant isotopic variant reaction by using the Chebyshev wave packet propagation method.[14–22] The related calculation results are presented in this paper. The rest of this paper is organized as follows. In Section 2, we present the theoretical method for obtaining the quantum dynamic information. In Section 3, we provide and discuss the computing results. Finally, we draw some conclusions from the present study in Section 4.

2. Theoretical method

In our calculations, we adopt the reactant Jacobi coordinates (R, r, γ), where R is the distance between the O^+ atom and the center of mass of the D_2 molecule, r is the D–D distance, and γ is the Jacobi angle between R and r. We express the Hamiltonian of this system as

$$\hat{H} = -\frac{1}{2\mu_R}\frac{\partial^2}{\partial R^2} - \frac{1}{2\mu_r}\frac{\partial^2}{\partial r^2} + \frac{(\hat{J}-\hat{j})^2}{2\mu_R R^2} + \frac{\hat{j}^2}{2\mu_r r^2} + V(R,r,\gamma) \quad (\hbar = 1), \tag{1}$$

*Project supported by the National Natural Science Foundation of China (Grant Nos. 11674198 and 11304185).

†Corresponding author. E-mail: qtmeng@sdnu.edu.cn

© 2018 Chinese Physical Society and IOP Publishing Ltd

where the μ_R and μ_r are the reduced mass relating to the two radial Jacobi coordinates R and r respectively, $V(R,r,\gamma)$ represents the potential energy of the ground electronic state, J denotes the total angular momentum, and the squared orbital angular momentum operator is expressed as

$$\hat{l}^2 = (\hat{J}-\hat{j})^2 = \hat{J}^2 + \hat{j}^2 - 2\hat{J}_z\hat{j}_z - \hat{J}_+\hat{j}_- - \hat{J}_-\hat{j}_+. \quad (2)$$

Here, $\hat{J}_z$ and $\hat{j}_z$ are the projections of $\hat{J}$ and $\hat{j}$ onto the body-fixed z axis, respectively, $\hat{J}_+$ ($\hat{J}_-$) and $\hat{j}_+$ ($\hat{j}_-$) are the corresponding raising (lowering) operators, which are responsible for the Coriolis coupling.[23]

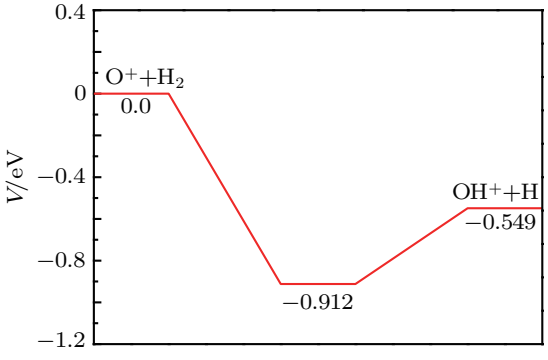


Fig. 1. (color online) Schematic PES of reaction $O^+(^4S)+H_2(X^1\Sigma_g^+) \rightarrow OH^+(X^3\Sigma^-)+H(^2S)$.

In the present study, we use the modified Chebyshev recursion[15] to propagate the initial wave packet

$$|\psi_{n-1}\rangle = D(2\hat{H}_{\text{scaled}}|\psi_n\rangle - D|\psi_{n-1}\rangle) \quad (n>1), \quad (3)$$

with $|\psi_1\rangle = D\hat{H}_{\text{scaled}}|\psi_0\rangle$ and $|\psi_0\rangle$ being the initial wave packets, which can be chosen as[18]

$$|\psi^{J_p}_{v_i j_i l_i}(R,r)\rangle = N\,\mathrm{e}^{-(R-R_{i0})^2/2\delta^2}\cos(k_{i0}R)\varphi_{v_i j_i}(r)\,|j_i l_i, J_p\rangle, \quad (4)$$

where k_{i0}, R_{i0}, and δ are the central momentum, the central position, and the width of the initial wave packet, respectively; N the normalization constant; v_i, j_i, and l_i are the initial vibrational, rotational, and orbital angular momentum quantum numbers, respectively; $\varphi_{v_i j_i}(r)$ is the vibrational eigenfunction of the reactant D_2. When dealing with the scattering problems by the time dependent quantum wave packet method, we always choose a damping function to enforce the outgoing boundary condition[14,15] at the grid edges. In our calculations, the absorption potential is defined as

$$D(R) = \begin{cases} 1, & (R \le R_d) \\ \mathrm{e}^{-d_R(R-R_d)^2}, & (R > R_d) \end{cases} \quad (5)$$

where R_d is the starting position of the absorption potential and d_R denotes the intensity of the absorption potential. The dynamic information is obtained just by the flux operator method, i.e., a surface is set to separate the channel of the product from the channel of reactant artificially, and the Fourier transform is used to analyze all the wave packets passing through the surface and then entering into the asymptotic region of the product channel to obtain the product distribution.

After the wave packet evolving with time is obtained, the related dynamic information can be acquired. To avoid calculating the S-matrix elements,[24,25] the total reaction probability is calculated using the following flux-based formula for the Chebyshev propagation:[26,27]

$$P(E) = \frac{1}{\pi\mu_r |a_i(E)|^2 (E_{\max}-E_{\min})^2 \sin^2\theta} \times \mathrm{Im}\left\langle \sum_k (2-\delta_{k0})\,\mathrm{e}^{-\mathrm{i}k\theta}\psi_k \middle| \sum_{k'}(2-\delta_{k'0})\,\mathrm{e}^{-\mathrm{i}k'\theta} \times \left[\delta(r-r_f)\frac{\partial}{\partial r}\psi_{k'}\right]\right\rangle, \quad (6)$$

where $r = r_f$ defines the dividing surface, which is the position of the flux calculated and θ is the Chebyshev angle. In the above equation, $a_i(E)$ is the amplitude of the initial wave packet, and its value is given by[28]

$$a_i(E) = \left\langle \mathrm{i}\sqrt{\frac{u_R k_i}{2\pi}} R h^{(2)}_\Lambda(k_i R) \middle| \psi_0 \right\rangle, \quad (7)$$

where $h^{(2)}_\Lambda(k_i R)$ is the spherical Hankel function of the second kind, Λ is given by $\Lambda(\Lambda+1) = J(J+1) + j_i(j_i+1) - 2\Omega^2$ with helicity quantum number Ω being the projection of the total angular momentum J on the body-fixed z axis in the Coriolis coupling calculation. In the reaction probability calculations, the Coriolis coupling effect is fully considered in a range of $0 < J \le 10$. For $J > 10$, to reduce the computing time, we cut the maximum helicity quantum number to $\Omega_{\max} = 10$. This value of $\Omega_{\max}$ provides convergent results of the reaction probabilities for the considered collision energy range.

The ICS can be given by summing the initial state-specified reaction probabilities for all J's partial waves,

$$\sigma_{v_i j_i}(E_c) = \frac{\pi}{(2j_i+1)k_i^2} \sum_{J,p,\Omega \le \min(J,j_i)} (2\hat{J}+1) P^{Jp}_{v_i j_i \Omega}(E_c), \quad (8)$$

in which k_i is equal to $\sqrt{2\mu_R E_c}$ with E_c being the collision energy.

3. Results and discussion

In this work, the extensive convergence tests have been performed for optimizing the numerical parameters. The obtained parameters are summarized in Table 1. We employ 300 and 200 equidistant grids for the R coordinate in a range of 0.01 a.u.–22.0 a.u. (The unit a.u. is short for atomic unit) and for the r coordinate in a range of 0.5 a.u.–14.0 a.u., respectively. For the Jacobi angle γ, 50 Gauss–Legendre quadrature points are taken between $\pi/2$ and π. In order to minimize the spectral range, both the potential and the kinetic energy[29] are truncated at 0.9 hartree (1 hartree $= 4.3597 \times 10^{-18}$ J). The

center of the initial packet is set to be $R_0 = 8.0$ a.u. with an average translational energy of 0.14 eV, and a width of 0.10 a.u. The starting position of the absorption potential is set to be $R_d = 16.0a_0$ and $r_d = 12.0a_0$ with absorption intensites $d_R = 0.0007a_0^{-1}$ and $d_r = 0.0005a_0^{-1}$, respectively. The position of flux calculated is placed at $11.9a_0$. As is well known, the propagation steps are very important for a convergent dynamic calculation. The convergence tests show that in this study the number of propagation steps in the range of collision energy up to 1.0 eV is 40000.

Table 1. Parameters of the quantum wave packet calculations (in atomic units, unless otherwise stated).

Parameter	Value
Grid/basis ranges and sizes	$R \in (0.01, 22.0)$, $(N_R = 300)$
	$r \in (0.5, 14.0)$, $(N_r = 200)$
	$\gamma \in (\pi/2, \pi)$, $(N_\gamma = 50)$
Absorption potential	$R_d = 16.0$, $d_R = 0.0007$
	$r_d = 12.0$, $d_r = 0.0005$
Initial wave packets	$R_0 = 8.0$, $E_0 = 0.14$ eV, $\delta = 0.10$
Spectral control (energy cut)	$E_{\rm cut} = 0.9$
Position of the flux calculated	$r_{\rm f} = 11.9$
Propagation steps	$N = 40000$

3.1. Reaction probabilities

The reaction probabilities of $O^+ + D_2 \rightarrow OD^+ + D$ reaction for five partial waves ($J = 0$, 20, 40, 60, 100) are displayed in Fig. 2. From this figure, we can observe the phenomena as follows. Firstly, the reaction probability of J=0 has no threshold energy, which is in agreement with the exothermic reaction. Secondly, because the potential well can induce the complex to form, all of the probabilities show oscillatory features in the whole range of collision energy, and the intensity of the oscillation is very strong in the low energy region, while it becomes less pronounced in the high energy region. Thirdly, comparing the titled reaction with the $O^+ + H_2$ reaction,[10] we find that because the mass of D_2 is greater than that of H_2, the reaction probabilities of the titled reaction are obviously smaller than those of the $O^+ + H_2$ reaction for all considered partial waves. Finally, we can find that, as a result of the centrifugal barrier increasing, the reaction threshold increases to the higher energy with the increase of J.

The vibrational excitation plays a significant role in a reaction, no matter whether the reaction is exothermic or endothermic. Figure 3 shows the reaction probabilities of the different vibrational states of the reactant D_2 for the titled reaction. As can be seen, the threshold energy of the reaction probability is equal to zero. Similarly because of the existence of the potential well in the reaction path, the oscillatory feature is displayed in the whole collision energy range for the reaction probabilities of different vibrational states. With the increase of the collision energy, the reaction curves of all the vibrational quantum numbers ($v = 0$, 1, 2) gradually decline. The vibrational states with $v = 1$, 2 for the reagent have a slight effect on the reaction, which is a little lower than ground vibrational state ($v = 0$) at low collision energies (< 0.3 eV), which means that the D_2 vibration does not enhance the reaction probability at low collision energies. The result is consistent with a previous study by Bulut *et al.*[12] However, we find that at the high collision energies (> 0.3 eV), the reaction probabilities of the vibrational states with $v = 1$, 2 obviously lie above that with $v = 0$ as shown in Fig. 3, which suggests that the raising of vibrational quantum number can accelerate the reaction.

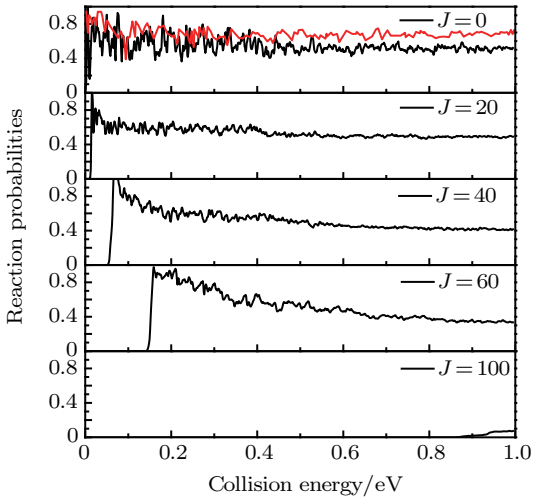


Fig. 2. (color online) The plots of reaction probability of the $O^+ + D_2$ ($v = 0$, $j = 0$) reaction for the total angular momentum $J = 0$, 20, 40, 60, 100. Black lines: $O^+ + D_2$; Red line: $O^+ + H_2$ ($J = 0$).

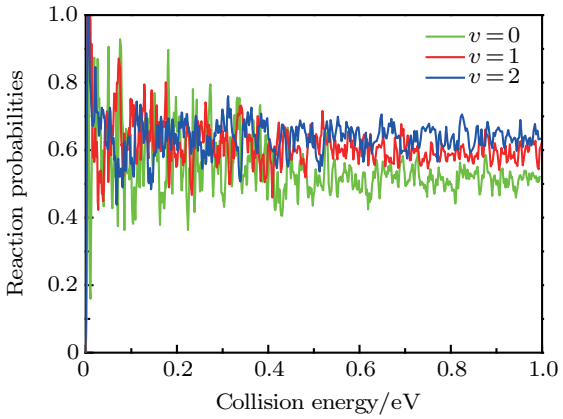


Fig. 3. (color online) The $J = 0$ reaction probabilities of the $O^+ + D_2(v, j = 0)$ reactions. Green line: $v = 0$; red line: $v = 1$; blue line: $v = 2$.

For the sake of getting the effects of the rotational excitation on the reaction, the reaction probabilities of the $O^+ + D_2$ ($v = 0, j$) reaction for $j = 0$, 1, 2 are plotted in Fig. 4. Obviously the reaction probabilities gradually decline with the collision energy increasing. From the three curves of $j = 0$, 1 and 2, it can be seen that the reaction probabilities of $j = 0$ lie above the others in the whole energy range due to the increase of the centrifugal barrier. Besides, we can find that the decrease of amplitude takes on a nonlinear relationship with the increase of j. This phenomenon indicates that the rotational

excitation of the reagent D_2 can impede the reaction, which is in excellent agreement with the conclusion obtained by Gao *et al.*[30] So we can come to the conclusion that the D_2 rotation will prevent the O^+ atom from coming close to the D_2 molecule for the exothermic and barrierless reaction.

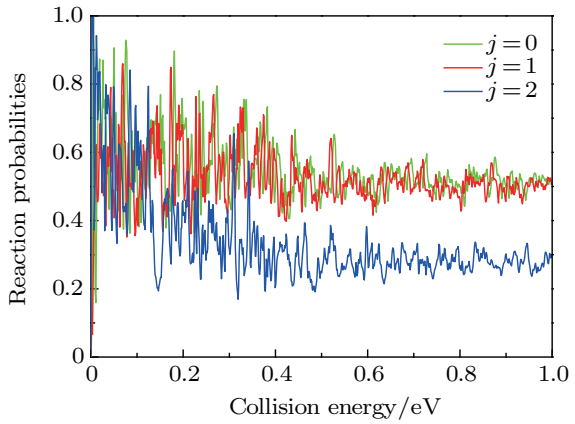


Fig. 4. (color online) Projects of $J = 0$ reaction probability versus collision energy of the $O^+ + D_2$ ($v = 0, j$) reactions. Green line: $j = 0$; red line: $j = 1$; blue line: $j = 2$.

3.2. Integral cross section

In order to test the convergence of this calculation for the titled reaction, the J-dependent partial wave contributions (weighted over a $2J + 1$ factor) to the ICS at the different collision energies are depicted in Fig. 5. We can see that for all curves of $E_c = 0.25$ eV, 0.5 eV, 0.75 eV, and 1.0 eV, the partial wave contribution increases with J at first. When the partial wave contribution rises to a highest value, it will decrease sharply with J increasing because of the increasing of the centrifugal potential. The oscillatory features of the curves are in agreement with the reaction probabilities of all partial waves. From the curves, it is clear that higher collision energy implies more partial waves contributing to the ICS. It can be seen that 104 partial wave contributions are enough to converge the ICS in the collision-energy range of 0.0 eV–1.0 eV.

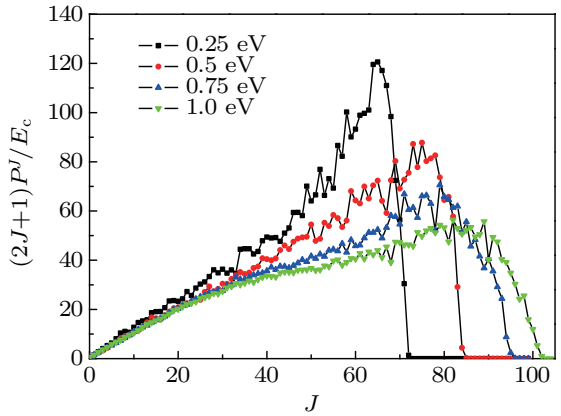


Fig. 5. (color online) Weighted partial wave contributions to the ICS at the different collision energies.

Through summing the partial waves and the reaction probabilities of different angular quantum numbers, we can obtain the ICS of the titled reaction, which is shown in Fig. 6 for the collision energy increasing up to 1.0 eV. From this figure we can find that the ICS not only shows no threshold due to the exothermal feature of the titled reaction, but also decreases with the collision energy increasing. In addition, the oscillatory character can be found in the low energy region, and it gradually vanishes as the collision energy increases. Figure 6 also shows the experimental results[4] of the ICS (300 K) for the titled reaction. Two blue dashed curves respectively represent the maximum and minimum values of the experimental data, which correspond to a 20% experimental error. We can obviously observe that the present ICS is in good agreement with the experimental results[4] within error margins, and only for $E_c < 0.05$ eV and $E_c > 0.8$ eV are the quantum results in the lower limit of the experimental data.

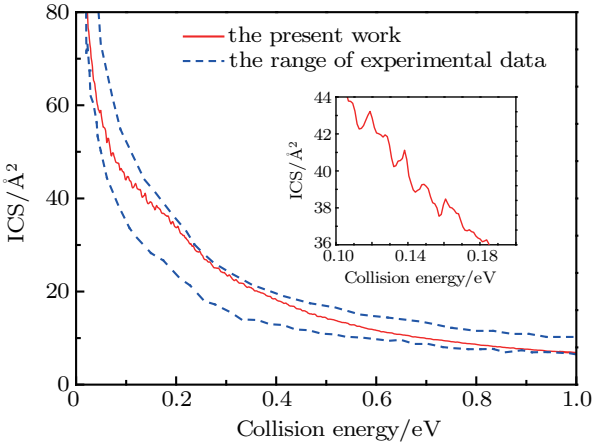


Fig. 6. (color online) Comparison of the present result with the experimental data for the $O^+ + D_2$ ($v = 0$, $j = 0$) reaction.

4. Conclusions

In this work, we acquire the quantum dynamic information of the $O^+ + D_2$ reaction based on a novel accurate global PES of the ground-state $H_2O^+(X^4A'')$ by the Chebyshev wave packet propagation method. Both the reaction probabilities and the ICS of the titled reaction in a collision energy range of 0.0 eV–1.0 eV are provided. The characteristics of the reaction probability curves are in accordance with those of the exothermic reaction with a potential well. Meanwhile it can be seen that the vibrational excitation of the reactant D_2 can promote the reaction, and the rotational excitation of the reactant D_2 can inhibit the reaction, due to the exothermic and barrierless reaction. The obtained ICSs are in excellent agreement with the existing experimental data, demonstrating the accuracy of the dynamical calculations.

Acknowledgment

The authors thank Prof. Shiying Lin of Shandong University for providing the computational code.

References

[1] Duley W W and Williams D A 1986 *Interstellar Chemistry* (New York: Academic press)
[2] Ng C Y 2002 *J. Phys. Chem. A* **106** 5953
[3] Fehsenfeld F C, Schmeltekopf A L, Goldan P D, Schiff H I and Ferguson E E 1967 *J. Chem. Phys.* **46** 2802
[4] Smith D, Adams N G and Miller T M 1978 *J. Chem. Phys.* **69** 308
[5] Burley J D, Ervin K M and Armentrout P B 1987 *Int. J. Mass Spectrom. Ion Processes* **80** 153
[6] Gioumousis G and Stevenson D P 1958 *J. Chem. Phys.* **29** 294
[7] Martínez R, Millań J and Gonzaález M 2004 *J. Chem. Phys.* **120** 4705
[8] Zhao J, Xu Y and Meng Q T 2009 *J. Phys. B: At. Mol. Opt. Phys.* **42** 165006
[9] Zhao J, Xu Y and Meng Q T 2010 *Chin. Phys. B* **19** 063403
[10] Martínez R, Sierra J D, Gray S K and González M 2006 *J. Chem. Phys.* **125** 164305
[11] Balint-Kurti G G 2004 *Adv. Chem. Phys.* **128** 249
[12] Bulut N, Castillo J F, Jambrina P G, Kłos J, Roncero O, Aoiz F J and Bañares L 2015 *J. Phys. Chem. A* **119** 11951
[13] Song Y Z, Zhang Y, Zhang L L, Gao S B and Meng Q T 2015 *Chin. Phys. B* **24** 063101
[14] Mandelshtam V A and Taylor H S 1995 *J. Chem. Phys.* **102** 7390
[15] Mandelshtam V A and Taylor H S 1995 *J. Chem. Phys.* **103** 2903
[16] Chen R Q and Guo H 1996 *Chem. Phys. Lett.* **261** 605
[17] Chen R Q and Guo H 1996 *J. Chem. Phys.* **105** 3569
[18] Gray S.K and Balint-Kurti G G 1998 *J. Chem. Phys.* **108** 950
[19] Wei W, Gao S B, Sun Z P, Song Y Z and Meng Q T 2014 *Chin. Phys. B* **23** 073101
[20] Lin S Y and Guo H 2006 *J. Chem. Phys.* **124** 031101
[21] Sun Z P, Lin S Y and Zheng Y J 2011 *J. Chem. Phys.* **135** 234301
[22] Tan R S, Zhai H C, Gao F, Tong D M and Lin S Y 2016 *Phys. Chem. Chem. Phys.* **18** 15673
[23] Chu T S and Han K L 2008 *Phys. Chem. Chem. Phys.* **10** 2431
[24] Neuhauser D, Baer, M, Judson R S and Kouri D J 1990 *J. Chem. Phys* **93** 312
[25] Zhang D H and Zhang J Z H 1994 *J. Chem. Phys.* **101** 1146
[26] Lin S Y and Guo H 2003 *J. Chem. Phys.* **119** 11602
[27] Meijer A J H M, Goldfield E M, Gray S K and Balint-Kurti G G 1998 *Chem. Phys. Lett.* **293** 270
[28] Althorpe S C 2001 *J. Chem. Phys.* **114** 1601
[29] Ma G B and Guo H 1999 *J. Chem. Phys.* **111** 4032
[30] Gao S B, Zhang J, Song Y Z and Meng Q T 2015 *Eur. Phys. J. D* **69** 111